



Design of functional multicomponent liquid crystalline mixtures with nano-scale pitch fulfilling deformed helix ferroelectric mode demands

Katarzyna Kurp^a, Michał Czerwiński^{a,*}, Marzena Tykarska^a, Peter Salamon^b, Alexej Bubnov^c

^a Institute of Chemistry, Military University of Technology, Gen. W. Urbanowicza str. 2, 00-908 Warsaw, Poland

^b Wigner Research Centre for Physics, Hungarian Academy of Sciences, Budapest, P.O.Box 49, H-1525, Hungary

^c Institute of Physics, The Czech Academy of Sciences, Na Slovance 1999/2, 182 21 Prague, Czech Republic

ARTICLE INFO

Article history:

Received 4 March 2019

Received in revised form 24 June 2019

Accepted 6 July 2019

Available online 12 July 2019

Keywords:

Ferroelectric liquid crystal

Multicomponent mixture

Polar smectic phase

Helical pitch

Self-assembling behaviour

Deformed helix ferroelectric mode

ABSTRACT

Design of new functional smectic liquid crystalline mixtures possessing polar behaviour remains quite highlighted task as those materials are highly requested by industry for specific applications in photonics. This work is devoted to specific practical method devoted to design of functional multicomponent ferroelectric liquid crystalline (FLC) mixtures based on chiral components exhibiting the ferroelectric and antiferroelectric polar order. The self-assembling behaviour, tilt angle, spontaneous polarization as well as dielectric properties of the prepared mixtures have been studied and discussed. The three resulting mixtures exhibit a broad range of the ferroelectric smectic phase, very low melting point, short helical pitch (below 180 nm) and relatively high tilt angle (about 40 degree). Excellent chemical stability and compatibility of components as well as moderate values of spontaneous polarization add another great deal to these FLCs materials for application in *deformed helix ferroelectric* mode in photonics and optoelectronics.

© 2019 Elsevier B.V. All rights reserved.

1. Introduction

It is difficult to overestimate the impact of the self-assembling materials on advances of the modern science and technology [1,2]. Chiral liquid crystals (LC) represent a specific class of organic materials, built up from the rod-like molecules, exhibiting self-orientation, which is possible to drive by an external stimulus like electric or magnetic field, light irradiation, and by mechanical stress. The presence of a polar layered ferroelectric or antiferroelectric structure of nanometre dimensions, characteristic to chiral LC materials, supplies the source of functionality and specific physical properties [2]. Advanced molecular design of new chiral structures can be a very influential and powerful tool to reach the properties desired by specific applications in opto-electronics and photonics. Specifically, the intermolecular interactions liable for the self-assembling can be precisely adjusted by building up the molecules from various units [3–9] or by design of binary/multicomponent

mixtures [10–13] or preparation of new LC nanocomposite materials [14–17].

Ferroelectric liquid crystals (FLC) fascinated many researchers all over the world for almost three last decades, in particular since N.A. Clark and S.T. Lagerwall demonstrated in 1980 [18] the fast switching electro-optical effect (SSFLC-Surface Stabilized Ferroelectric Liquid Crystals) based on the properties related to ferroelectric polar smectic structure. FLCs are very promising competitors of nematic liquid crystals due to their faster response times with a reasonably lower driving voltage. During recent years, FLC materials are still extensively studied [5–9,12–13,19–22]. However, especially for photonic applications, the very important continuously tuneable threshold-free phase shift is not offer by the SSFLC effect. In this case, *deformed helix ferroelectric* (DHF) liquid crystals mode is very promising because of tuneable, continuous and hysteresis-free optical phase shift at low voltages and short response time [23–31] either in transmission or in reflection mode [32]. The DHF effect appears in chiral LC materials forming a helical structure. The helix axis is parallel to the substrates' plane of electro-optical cell and it is tilted after applying electric field E (which should be lower than the critical field E_C of the helix unwinding). The transmission (T), switching time (τ) and critical electric field (E_C),

* Corresponding author at: Faculty of Advanced Technologies and Chemistry, Military University of Technology, Gen. W. Urbanowicza Str. 2, 00-908 Warsaw, Poland.

E-mail address: michal.czerwinski@wat.edu.pl (M. Czerwiński).

which characterize DHF mode, can be described by the following equations [31]:

$$T_h = \sin^2 2[\beta \pm \Delta\alpha(E)] \cdot \sin^2 \frac{\pi d_{FLC} \Delta n_{eff}(\lambda, f, E)}{\lambda} \quad (1)$$

$$\tau = \frac{\gamma_\varphi p_0^2}{K 4\pi^2} \quad (2)$$

$$E_c = \frac{\pi^4 K}{4 P_s p_0^2} \quad (3)$$

where: β is the angle between the polarizer and helix axis of the ferroelectric phase; $\Delta\alpha$ denotes the shift of helical axis due to electric field; Δn_{eff} is the effective birefringence and λ is the wavelength; γ_φ is the rotation viscosity; K is the elastic constant, p_0 is the helical pitch length; P_s is the spontaneous polarization. From Eqs. (1)-(3) it is clearly follow that one of the most important material parameter (as it strongly affects τ and E_c in DHF) is the helical pitch length, which should be as low as possible (at least below 200 nm). High tilt angle (ideally as close to 45° as possible) promoting high transmission and a moderate spontaneous polarization (ideally within range 120–180 nC/cm²) are further very important and required features. This is truly so as on the one hand low values of spontaneous polarization results in a strong decrease of contrast, and on the other hand high P_s values cause the shortening of electric field range in which DHF effect appears.

Recently, an alternative method [33] to obtain FLC materials responding the requirements of DHF mode has been shown. It is based on smart mixing of exclusively chiral compounds in a specific proportion in which the competition and frustration between the ferroelectric and antiferroelectric polar order exists and that in turns is beneficial for obtaining V-shape electro-optical switching [34,35] (important feature in DHF mode). Due to that we obtained the best mixture (with acronym **W-212B3A**) with almost appropriate properties but exhibiting also two specific disadvantages that are still needed to be resolved. The first one is associated with a possible instability that might occur in a mixture based on components with different molecular structure. Another one is too high values of spontaneous polarization which, according to Eq. (3), considerably decrease the value of E_c . Furthermore, our basic research [3] confirms that two ring compounds with a very low melting point and the absence of any liquid crystalline behaviour can effectively decrease the helical pitch while mixing with FLC materials. On the other hand, two ring compounds exhibiting the SmA* phase cause unwinding of the helix in FLCs [3].

The main objective of this work is to achieve optimum effectiveness of DHF effect by design of several new ferroelectric liquid crystalline mixtures, based on the method described above. The designed mixtures are expected (i) to fulfil almost all material requirements for DHF mode and (ii) to be consisted of structurally similar compounds that can cause the required tunability of spontaneous polarization and helical pitch length values.

2. Experimental

The phase transition sequence was determined from the textures and their changes on planar cells (where the long axes of molecules are oriented parallel to the substrates), using polarizing optical microscope (Nikon Eclipse E600POL, Nikon, Tokyo, Japan). The planar cells (AWAT company, Warsaw, Poland) in bookshelf geometry (where the smectic molecular layers are oriented uniformly) for texture observations and electro-optical studies were made from glass with transparent electrodes of indium tin-oxide (ITO) (5 × 5 mm²), separated by Mylar® sheets defining the cell thickness (12 μm thick). The sample cells were filled with the studied FLC mixtures in the isotropic phase by the capillary action. The Linkam LTS E350 (Linkam, Tadworth, UK) heating/

cooling stage equipped with a TMS 93 temperature controller was used, enabling temperature stabilization within ±0.1 °C. Dependencies of phase transition temperatures upon mass fraction of components are presented.

The measurements of the spontaneous polarization, tilt angle as well as switching ON time (τ_{10-90}) have been done on similar planar samples. Values of the spontaneous polarization, P_s , have been determined from the current measurements with a triangular electric field switching at a frequency of 50 Hz and an applied electric field magnitude of 20 V/μm. A specific software for automation of the spontaneous polarization measurements has been developed and used. Tilt angle, θ_s , has been determined optically under the applied d.c. electric field ±10 V/μm, by measuring the angular difference between the extinction positions of the unwound structures under fields of opposite polarity. Values of the spontaneous polarization, tilt angle and switching ON time have been measured on cooling.

The helical pitch measurements were performed based on the selective light reflection phenomenon. Before measurements, a thin layer of orienting surfactant was applied on the glass plate to force the required homeotropic alignment (perpendicular to the surface) of the molecules of liquid crystal. Such slides were used to register a baseline on a UV-Vis-NIR spectrophotometer (SHIMADZU 3600) in the wavelength range 360–3000 nm. After baseline collection, the tested mixtures were applied on the surface of the slide and the spectra were recorded. The measurements were performed in a cooling cycle. The spectrophotometer was equipped with a U7 MLW temperature controller. More details on helical pitch measurements can be found in Ref. [36]. Helical pitch length, p , was calculated from the equation $p = \lambda_s / 2n_{av}$ for the SmC* phase where λ_s is the wavelength of selectively reflected light from periodic structure and n_{av} is average refractive index (the value of $n_{av} = 1.5$ has been taken for calculation according to Ref. [37]). Dependencies of helical pitch upon temperature are presented.

The helix handedness was measured by polarimetry method [38]. The homeotropically aligned sample was observed in transmission between crossed polarizers and the top polarizer was rotated with respect to the bottom one. The analysis of the transmitted light was performed by polarizing optical microscopy (POM). According to the convention described in Ref. [39] a clockwise rotation of analyzer, in order to produce the darkest state (or minimum transmission state) when observation is made toward the coming beam, indicates a *dextro* or left-handed helix and anticlockwise rotation indicates a *levo* or right-handed helix. The temperature of the helix twist inversion was established by the analysis of transmitted light versus temperature of a homeotropically aligned sample observed in POM; the brightest texture indicates the fully unwound structure [39].

The frequency dispersion of complex permittivity ($\varepsilon^* = \varepsilon' - i\varepsilon''$) has been measured within the temperature range of the SmA* and SmC* phases on cooling, using a Schlumberger 1260 impedance analyzer in the frequency range of 1 Hz ÷ 1 MHz keeping the temperature stable during the frequency sweep within ±0.1 K. The measurements have been performed under zero d.c. bias voltage. The frequency dispersion data have been analysed using the generalized Cole-Cole formula for the frequency dependent complex permittivity extended by the second term to eliminate the low frequency contribution:

$$\varepsilon^* - \varepsilon_\infty = \frac{\Delta\varepsilon}{1 + (if/f_r)^{(1-\alpha)}} - i \frac{\sigma}{2\pi\varepsilon_0 f^n} \quad (4)$$

where f_r is the relaxation frequency, $\Delta\varepsilon$ is the dielectric strength, α is the Cole-Cole distribution parameter, ε_0 is the permittivity of the vacuum and ε_∞ is the high frequency permittivity, σ is the d.c. conductivity and n is a parameter of fitting. The measured real, $\varepsilon'(f)$, and imaginary, $\varepsilon''(f)$, parts of complex permittivity were fitted

simultaneously using specific software “Scientist” from MicroMaths Scientist Software Corporation. For selected representative mixtures, the dependencies of relaxation frequency and dielectric strength upon temperature are presented.

3. Results and discussion

Here, the description of the multicomponent mixture design together with detailed characterization of the selected ferroelectric liquid crystalline mixtures are presented. Specifically, the phase diagrams, composition of the best mixtures, together with the spontaneous quantities (namely the spontaneous polarization, tilt angle determined optically, helical pitch length) and dielectric properties for the functional FLC mixtures are shown and discussed.

3.1. Mixture design and mesomorphic behaviour

The chemical formulae together with the mesophase sequences and phase transition temperatures on heating cycle of original pure chiral components used for design multicomponent mixtures are presented in Table 1. The precise weight composition of the resulting mixtures is also shown in Table 1. All components possess the same chiral terminal chain; the non-chiral terminal chain differs in number of carbon and fluorine atoms. Other differences are related to the structure of the rigid molecular core. All tested

compounds are chiral esters with biphenyl benzoate or phenyl biphenylate, or benzoate rigid core; further tuning of the molecular structure was reached by lateral substitution by fluorine atom at the specific place in the rigid core. Tuning the concentration of those structurally similar compounds with above mentioned fine differences in the molecular structure effectively allow us to adjust the required features of resulted designed multicomponent mixture. Sequence of phases and phase transition temperatures of resulted multicomponent mixtures are presented and summarised in Table 2.

3.2. Design and characterization of W-212C mixture

In Ref. [33] the ferroelectric **W-212B** mixture was presented. Its composition is shown in Table 1. It consists of three three-ring esters (compounds **1**, **2** and **3**) mixed in proper ratio (1:1:2), respectively. This compounds provide a stable SmC* phase with very high tilt angle value and short helical pitch. Two-ring compounds **4** and **5**, forming the SmA* phase, are added as further functional components in order to decrease the melting temperature of the resulting mixture. This mixture was modified to obtain a material useful for DHF electro-optic effect. The modifications of **W-212B** mixture presented in Ref. [33] allowed us to decrease considerably the helical pitch length but at the same time caused too strong increase of the spontaneous polarization (above 180nC/cm² below

Table 1
Chemical structures, phase transition sequences and temperatures (in heating cycle) [°C] of chiral components used for design of **W-212B** [33], **W-212C**, **W-212C2** and **W-212C3** mixtures.

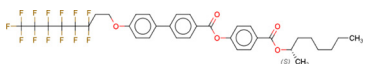
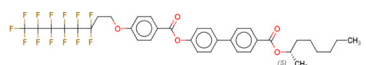
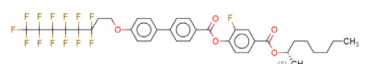
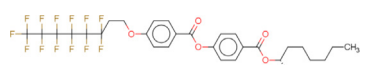
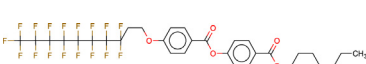
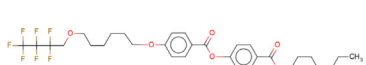
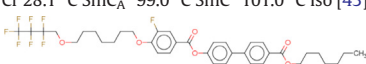
No.	Chemical structure and phase sequence of used compounds	Mixtures acronyms			
		W-212B	W-212C	W-212C2	W-212C3
		Concentration (wt%)			
1	 Cr _{II} 80.7 °C Cr _I 98.9 °C SmC* 141.4 °C SmC _α * 149.0 °C SmA* 184.0 °C Iso [40–42]	11.88	8.35	7.52	7.52
2	 Cr _{II} 94.3 °C Cr _I 97.9 °C SmC* 155.6 °C SmA* 184.6 °C Iso [40–42]	12.13	8.31	7.48	7.48
3	 Cr 89.7 °C SmC* 133.6 °C SmC _α * 134.8 °C SmA* 154.7 °C Iso [40–42]	24.29	18.54	16.69	16.69
4	 Cr 60.0 °C SmA* 63.4 °C Iso [3]	38.80	29.75	26.77	26.77
5	 Cr 82.2 °C SmA* 90.7 °C Iso [3]	12.90			
6	 Cr 36.2 °C Iso [3]	–	35.05	31.54	31.54
7	 Cr 28.1 °C SmC _A * 99.0 °C SmC* 101.0 °C Iso [43]	–	–	10.00	5.25
8	 Cr 37.4 °C SmC _A * 103.1 °C SmC* 104.3 °C SmA* 109.1 °C Iso [43]	–	–	–	4.75

Table 2

Sequence of phases and phase transition temperatures (on heating cycle) [°C] for *W-212B* [33], *W-212C*, *W-212C2* and *W-212C3* mixtures.

Mixture	Cr	T	SmC*	T	SmA*	T	Iso
<i>W-212B</i>	•	11.4	•	83.9	•	118.0	•
<i>W-212C</i>	•	<−10.0	•	61.8	•	97.0	•
<i>W-212C2</i>	•	<−10.0	•	61.7	•	71.0	•
<i>W-212C3</i>	•	<−10.0	•	64.4	•	74.7	•

30 °C). This drawback of mixture *W-212B* motivated our present studies looking for further improvements. The newly designed *W-212C* mixture was formulated in such a way that compound **5** was exchanged by a non-mesogenic compound **6**, with much lower melting point and a strong tendency to decrease helical pitch. Due to that the SmA*-SmC* phase transition as well as melting point of *W-212C* mixture is much lower than that of *W-212B* mixture. Furthermore, and importantly, the helical pitch length has been decreased significantly for *W-212C* mixture in comparison to *W-212B* as shown in Fig. 1a. The above mentioned results are very consistent with our previous investigation of miscibility and helical parameters in binary LC systems [3]. Adding compound **6** to the base compound (in this paper it is compound **1**) results in a slight decrease of helical pitch value; the SmC* phase exists up to 0.4 mol fraction of two-ring compound **6** in binary mixtures. Moderate values of the spontaneous polarization (see Fig. 1b) as well as relatively high values of the tilt angle (Fig. 1c) are additional important advantages of *W-212C* mixture.

3.3. Fine tuning of the composition and behaviour of *W-212C* mixture

Based on results from our previous work [33], compound **7** and eutectic mixture of compound **7** and **8** (denoted as *W-1000*) were chosen for fine tuning of the behaviour of *W-212C* mixture.

Two systems, namely *W-212C* + compound **7** as well as *W-212C* + *W-1000*, were prepared in order to obtain a proper composition possessing the frustrated ferroelectric phase [34,35]; this has been done analogically to our previous work [33]. Phase diagrams of those systems are shown in Fig. 2.

Developed several years ago, *W-1000* mixture is eutectic, bicomponent mixture containing two antiferroelectric compounds (denoted here as **7** and **8**), which possesses on heating the following mesophase sequence: Cr-SmC_A*-SmC*-SmA*-Iso. This mixture is quite highlighted as it exhibits typical orthoconic behaviour which was established recently [44–47]. Whereas *W-212C* mixture is composed from different compounds, namely **1–4** and **6**, as well as it has a similar phase sequence: Cr-SmC*-SmA*-Iso; the antiferroelectric phase is absent. The stability of antiferroelectric phase in system *W-212C* + *W-1000* is very high (see Fig. 2b) and the destabilization occurs at a very low mass fraction of *W-1000* mixture. System containing up to 0.85 mass fraction of *W-212C* mixture still exhibits the antiferroelectric phase at low temperatures. Mixture composition 0.1 + 0.9 mass fraction, for *W-1000* and *W-212C*, respectively, forms the frustrated SmC* phase. In *W-212C* + Compound **7** system, the stability of the SmC_A* phase is comparable to the mentioned case (see Fig. 2a). Taking into account the predictions (specifically due to *W-1000* mixture that contains 52.5 wt% of compound **7**) only mixtures containing up to 0.4 mass fraction of compound **7** in

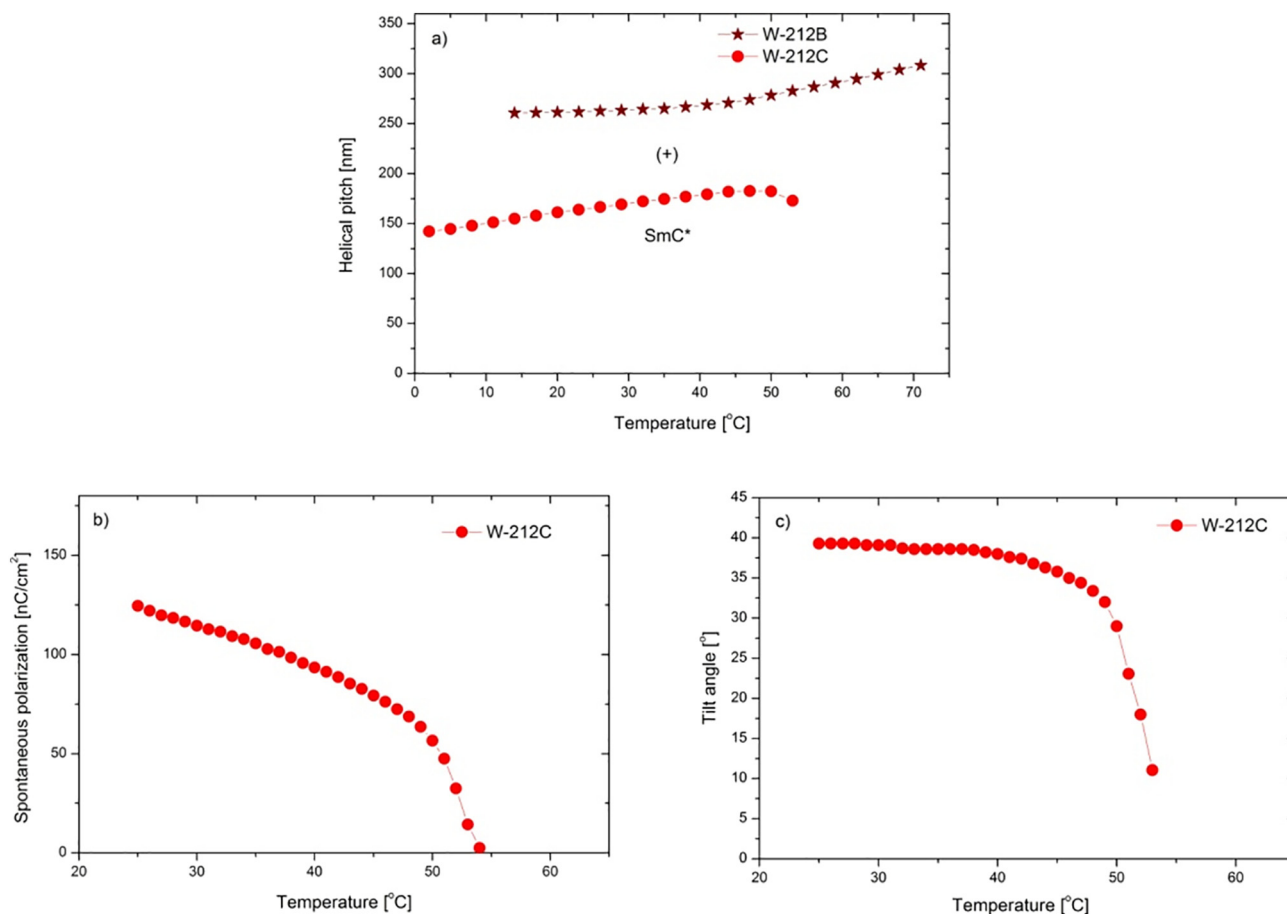


Fig. 1. Temperature dependence of: (a) the helical pitch length for multicomponent *W-212B* [33] and *W-212C* mixtures; (b) spontaneous polarization and (c) tilt angle determined optically for *W-212C* mixture. Sign "+" indicates the right handedness of the helix.

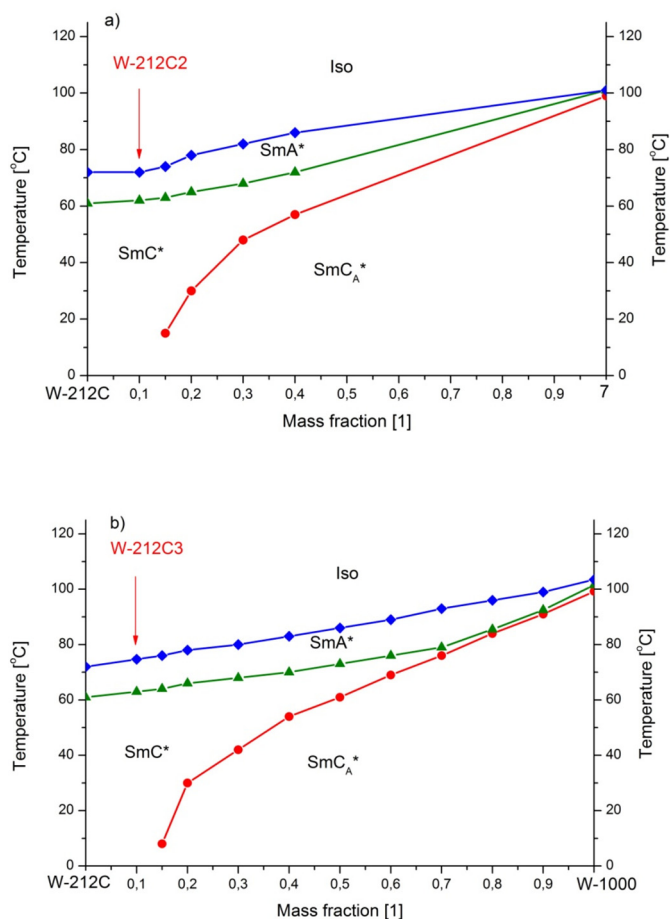


Fig. 2. Phase diagrams for two systems: (a) *W-212C* + **compound 7** and (b) *W-212C* + **W-1000**. Vertical arrows indicate the specific composition for the resulting *W-212C2* and *W-212C3* mixtures.

W-212C mixture were prepared. Antiferroelectric phase appears above 0.15 mass fraction of **compound 7** in *W-212C* mixture. Similarly, as for the previous system, mixture with 0.1 mass fraction of **compound 7** in *W-212C* mixture possesses only the SmC^* phase with the broadest temperature range. In comparison to the multicomponent mixtures from *W-212B* series [33], a replacement of one component, which formed the SmA^* phase, by another component which does not exhibit any LC behaviour will allow to stabilise the antiferroelectric SmC_A^* phase in a much broader concentration range.

The results of helical pitch measurements as a function of temperature and of the temperature relative to the SmC^* - SmC_A^* phase transition obtained for *W-212C* + **compound 7** and *W-212C* + **W-1000** systems are given in Fig. 3a and b as well as in Fig. 4a and b, respectively. In order to compare helical pitch values in the ferroelectric phase, the enlarged areas of the results are shown in Fig. 3c and 4c for both systems.

Compound 7 is characterized by the presence of right-handed helix in SmC^* phase, while in the SmC_A^* phase, right and left handedness were observed at the lower and the higher temperature range, respectively (see Fig. 3a). The temperature of helix twist sense inversion of pure **compound 7** is equal to 52 °C. The multicomponent *W-212C* mixture forms only right-handed helix in the entire temperature range of SmC^* phase. Increasing the quantity of **compound 7** in *W-212C* mixture causes substantial decrease of helical pitch value for left-handed helix in the SmC_A^* phase (see Fig. 3a and b). Macroscopic helical structure in the synclinal

ferroelectric phase was determined to be right-handed for all mixtures. The lowest value of helical pitch in a broad temperature range was found for *W-212C* mixture containing 0.1 mass fraction of **compound 7**. However, *W-212C* mixture possesses the shortest helical pitch below room temperature.

The *W-1000* mixture consists 52.5 wt% of **compound 7**, therefore its dependence of helical pitch upon temperature is similar: right handedness at low temperature and left handedness at higher temperature range of the SmC_A^* phase (see Fig. 4a). Mixtures from system *W-212C* + *W-1000* with 0.15–0.8 mass fractions of *W-1000* mixture are characterized by the presence of right-handed helix in the SmC^* phase and left-handed helix in the SmC_A^* phase. The temperatures of helix twist sense inversion of *W-1000* mixture as well as of *W-212C* with 0.8 mass fractions of *W-1000* mixture are equal to 52 °C and 23 °C, respectively. An increase of *W-1000* mixture concentration in *W-212C* mixture causes the appearance of SmC_A^* phase (for 0.15 mass fraction) and considerable increase of helical pitch for left-handed helix in this phase (see Fig. 4a and b). The helical structure in the ferroelectric phase was found to be right-handed for all compositions. Both the base *W-212C* mixture and the *W-212C* mixture containing 0.1 mass fraction of *W-1000* mixture exhibit the lowest nano-scale values of helical pitch (about 140 nm below room temperature).

3.4. Advanced characterization of resulting *W-212C2* and *W-212C3* mixtures

Base *W-212C* mixture and mixture in which the frustrated ferroelectric phase exists (*W-212C2* and *W-212C3*, marked in red on phase diagrams in Fig. 2a and b, respectively) were chosen for further investigations. Those mixtures possess a quite low melting point (below -10 °C), relatively broad temperature range of the ferroelectric phase (more than 70 degree) and reasonable temperature range of the paraelectric SmA^* phase above the SmC^* phase.

Temperature dependence of helical pitch length for *W-212C*, *W-212C2* and *W-212C3* mixtures are shown in Fig. 5 within the SmC^* phase. When pure **compound 7**, which forms left- and right-handed antiferroelectric phase, is added to the multicomponent ferroelectric *W-212C* mixture, then the value of helical pitch is decreased in higher temperature region (above 29 °C) and increased in lower temperature region in comparison to values of helical pitch for *W-212C* mixture (see *W-212C2* in Fig. 5). Interestingly, when two **compounds 7** and **8** (components of mixture *W-1000*) are added to *W-212C* mixture, only a slight increase in the length of the helical pitch in low temperature region is observed (see *W-212C3* in Fig. 5). The value of helical pitch length is lower than 180 nm for all designed mixtures, although the dependence is slightly growing with temperature. As the values of helical pitch length for *W-212C2* mixture are the highest from all three investigated mixtures, further studies were performed for *W-212C* and *W-212C3* mixtures only.

The temperature dependence of the spontaneous polarization $P_s(T)$ and tilt angle $\theta_s(T)$ for *W-212C* and *W-212C3* mixtures have been measured and are presented in Fig. 6 and Fig. 7, respectively.

The lowest value of spontaneous polarization was detected for the base *W-212C* mixture, which contains the highest quantity of ferroelectric compounds; components with antiferroelectric phase are absent for this mixture (see Table 1). On the other hand, antiferroelectric components of *W-1000* mixture caused slightly faster saturation of the tilt angle values (about 40 degree) with temperature decrease in *W-212C3* mixture (Fig. 7).

The temperature dependence of the rotational viscosity γ_{rot} was evaluated from the measurements of the switching ON time (τ_{10-90}) while driving with a square driving pulse at saturated

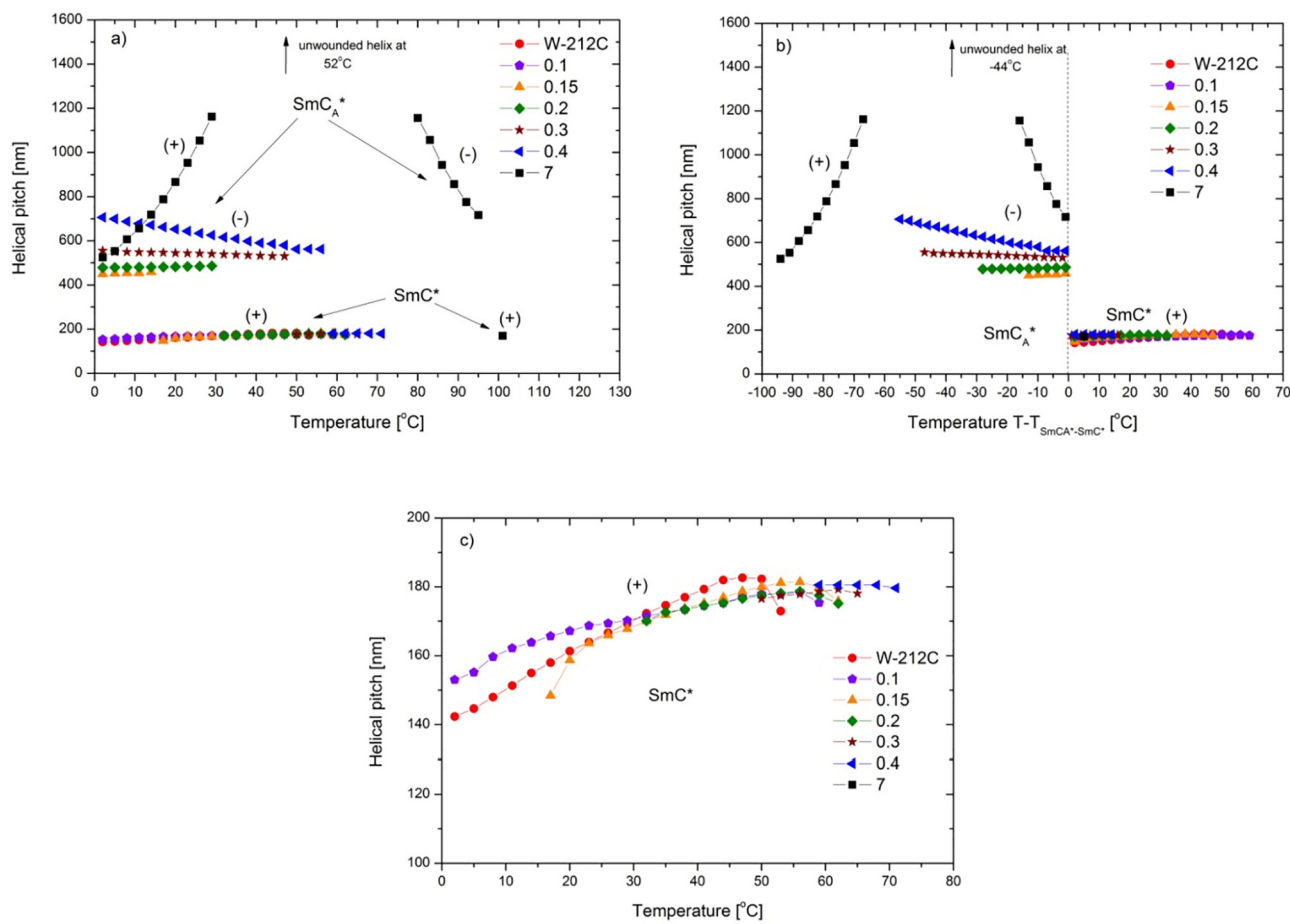


Fig. 3. Dependence of helical pitch length versus temperature (a) and versus temperature relative to the $\text{SmC}^*-\text{SmC}_A^*$ phase transition (b) for **W212C + compound 7** system. Enlarged area of the helical pitch's temperature dependence within the SmC^* phase is shown in (c). Arrows of the corresponding colour indicate the temperatures at which the helix became fully unwound. The sense of the helical twist is indicated by "+" for the right-handed helix and by "-" for the left-handed helix.

voltage (Fig. 8a, b). It was calculated using semiempirical formula [48]:

$$\gamma_\varphi = \frac{1}{1,8} P_S E \tau_{10-90} \quad (5)$$

where: $E = U/d$, U denotes the applied voltage, d stands for the cell gap.

Mixture **W212C** and **W212C3** are characterized by switching On time a little above 100us around room temperature, as it is clear visible in Fig. 9a. What is more important for switching times in DHF mode according to the Eq. (2), both investigated mixtures exhibit rotational viscosity in the range 1–1.8 Pa-second. Such values are two times higher than for the newest materials used in DHFLC [31]. However, mixtures **W212C** and **W212C3** exhibit melting points much lower than described in [31].

Broadband dielectric spectroscopy was done on two resulting mixtures, namely for **W212C** and **W212C3**. The real, ϵ' , and imaginary parts, ϵ'' , of complex permittivity for **W212C** mixture versus temperature and versus frequency are presented in Fig. 9a and b as an illustrative result to confirm the ferroelectric character of the polar phase. Dielectric spectra obtained within the whole temperature range of the ferroelectric SmC^* phase at zero bias electric field reveal a strong contribution of the Goldstone mode (the relaxation mode related to azimuthal fluctuations of the molecules in the smectic layer). In the vicinity of the $\text{SmA}^*-\text{SmC}^*$ phase

transition, a collective mode related to the molecular fluctuations in the tilt magnitude, the so-called soft mode, was detected. The measured data were fitted by the Cole-Cole formula (Eq. (4)) for the frequency-dependent complex permittivity. The temperature dependence of the fitted relaxation frequency, $f(T)$, and the dielectric increment, $\Delta\epsilon(T)$, are shown in Fig. 10a and b for the whole temperature range of the SmA^* and SmC^* phases. This behaviour fully confirms the ferroelectric character of the SmC^* phase detected for the tested mixtures. The relaxation frequency of the mode is slightly decreasing with temperature decrease, while the dielectric strength is continuously decreasing until the crystallisation occurs. This is quite typical behaviour of the Goldstone mode at the ferroelectric SmC^* phase [5,7,9]. Detailed discussion on the specific behaviour of all detected modes, revealed by the broad-band dielectric spectroscopy, with respect to the mixture composition is beyond the scope of the present work and will be presented elsewhere.

4. Conclusions

Three multicomponent mixtures with broad range of the ferroelectric smectic phase, very low melting point, nano-scale helical pitch below 180 nm, high tilt angle and moderate spontaneous polarization have been designed. One of the resulted mixtures is based on compounds possessing the ferroelectric SmC^* phase, the orthogonal SmA^* phase or without mesophases. Two other mixtures have

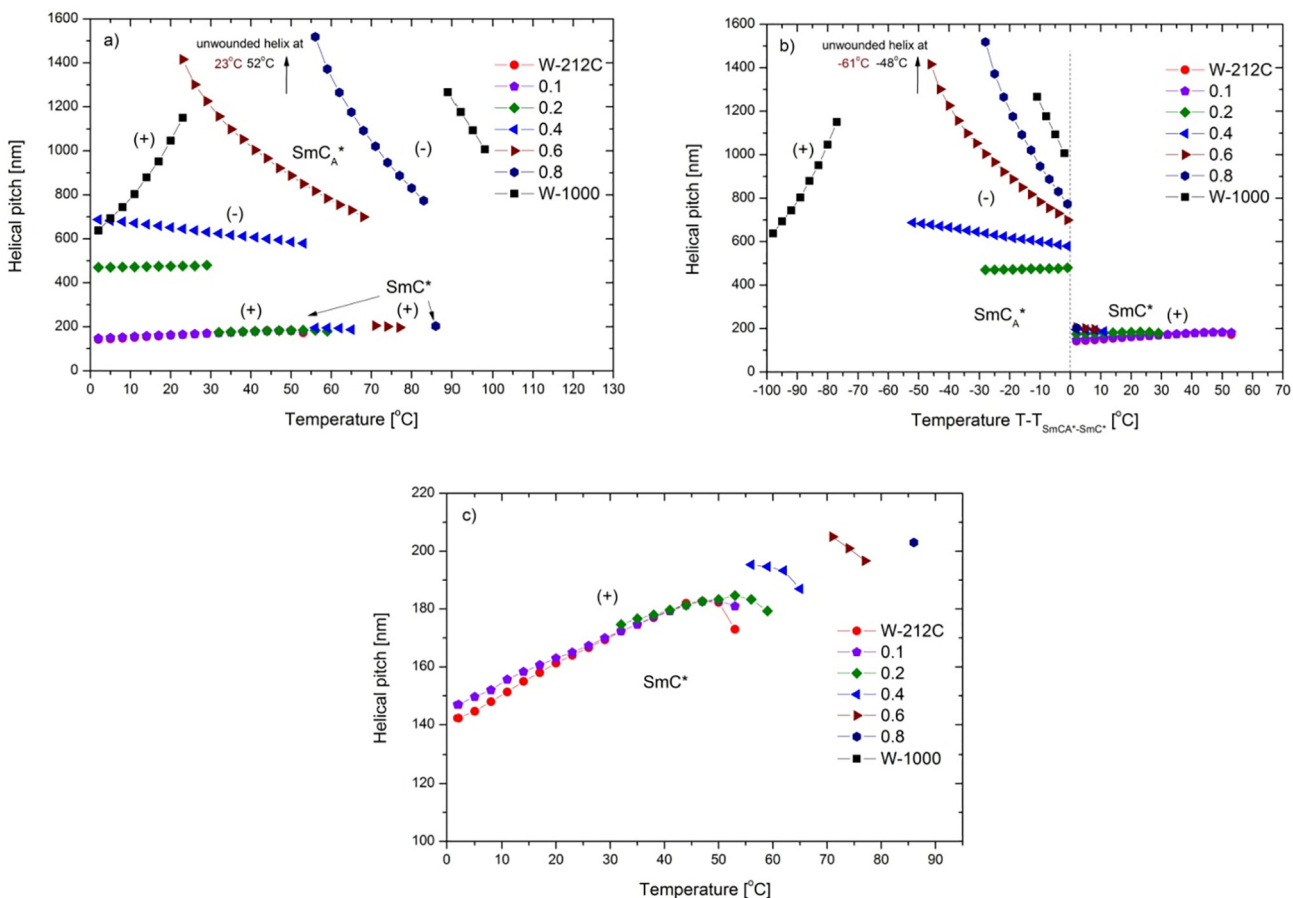


Fig. 4. Dependence of helical pitch length versus temperature (a) and versus temperature relative to the $SmC^* - SmC_A^*$ phase transition (b) for $W-212C + W-1000$ mixture system. Enlarged area of temperature dependence of helical pitch in the SmC^* phase is shown in (c). Arrows of the corresponding colour indicate the temperatures at which the helix became fully unwound. The sense of the helical twist is indicated by “+” for the right-handed helix and by “-” for the left-handed helix.

been developed using the method in which the frustrated ferroelectric phase has been obtained. Such approach gives opportunity to tune the specific features of final mixture by changing the concentration and the type of mixing components as well as unite and even enhance the ferroelectric and antiferroelectric properties of

the used components. Furthermore, some mixtures from two designed binary systems ($W212C + W1000$ and $W-212C + \text{compound 7}$) possess antiferroelectric phase with a very short and simultaneously temperature independent helical pitch that make them potentially useful for deformed helix antiferroelectric liquid

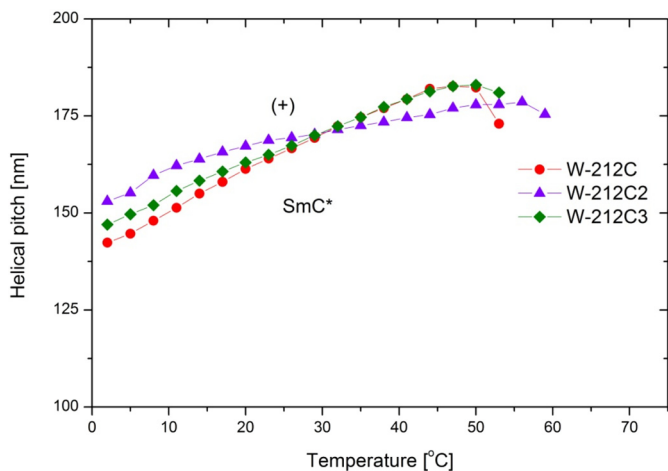


Fig. 5. Temperature dependence of helical pitch length for $W-212C$, $W-212C2$ and $W-212C3$ mixtures as indicated. Sign “+” indicates the right-handedness of the helix.

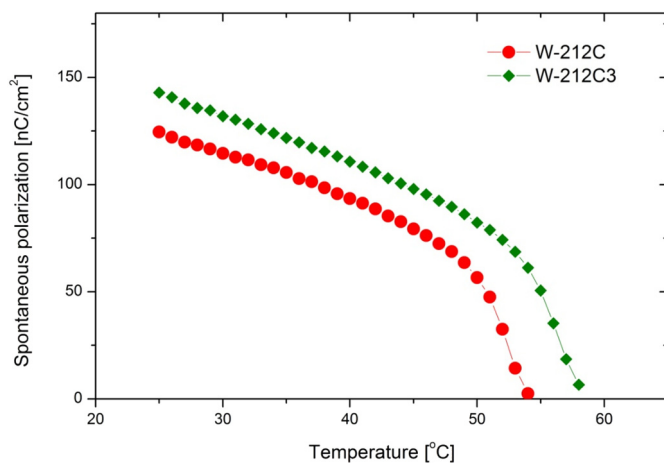


Fig. 6. Temperature dependence of the spontaneous polarization, P_s , for $W-212C$ and $W-212C3$ mixtures.

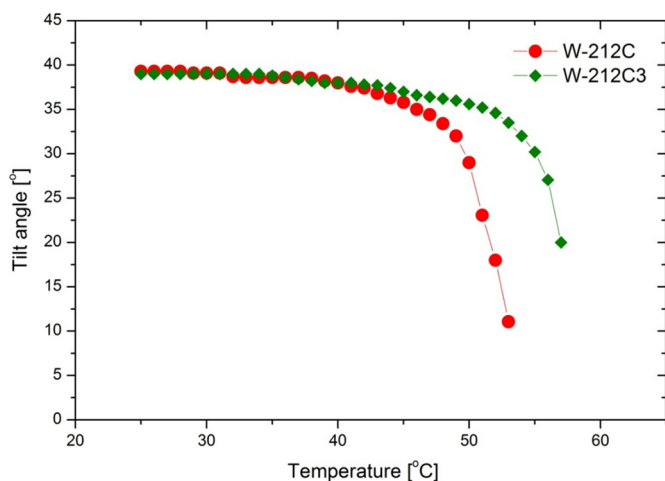


Fig. 7. Temperature dependence of the tilt angle, θ_s , measured optically for **W-212C** and **W-212C3** mixtures.

crystal (DHAFLC) effect, recently shown by Pozhidaev et al. [49]. Taking into account basic necessities, the designed mixtures fulfilled almost all material requirements for DHF mode, including

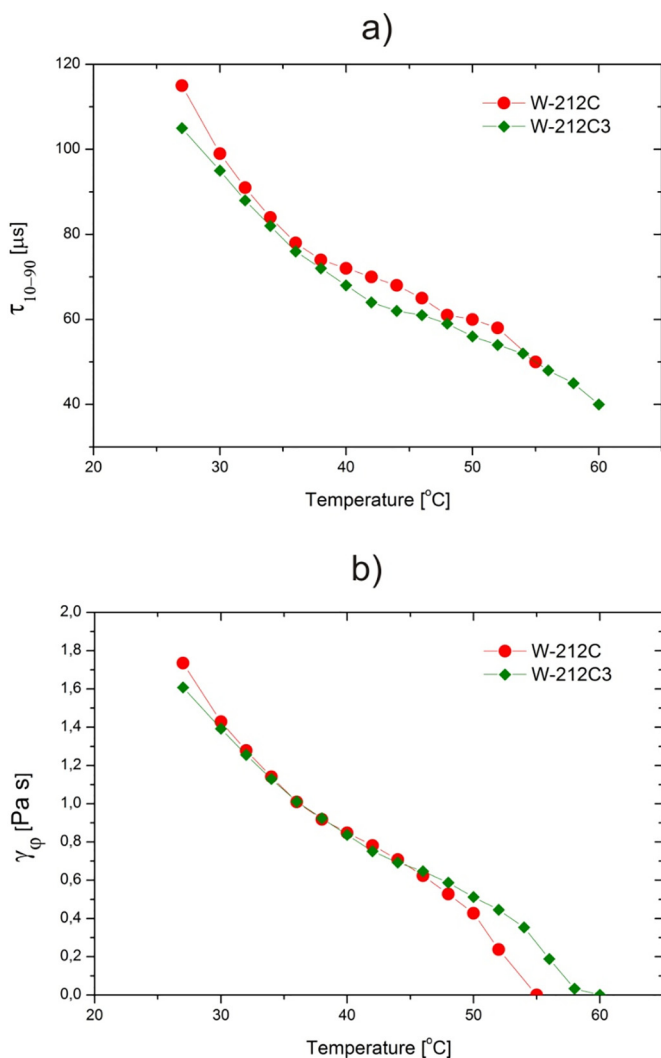


Fig. 8. Temperature dependence of (a) the switching ON time and (b) the rotational viscosity for **W212C** and **W212C3** mixtures as indicated.

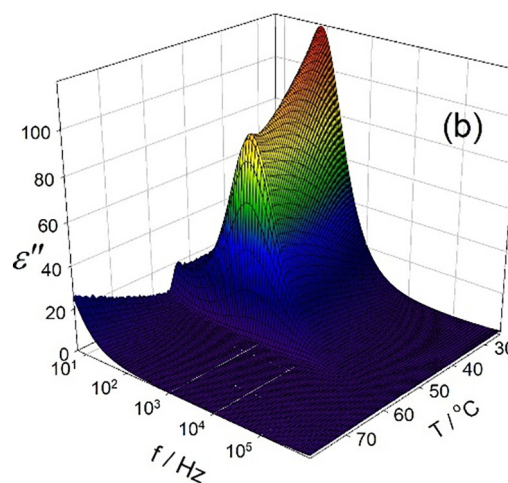
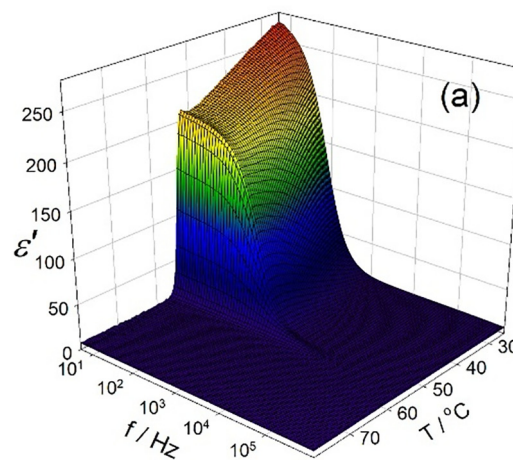


Fig. 9. 3D-plots of real ϵ' part (a) and imaginary, ϵ'' , part (b) of complex permittivity at zero bias electric field measured on a 12 μm thick sample cell for **W212C** mixture within the temperature range of the paraelectric SmA* and the ferroelectric SmC* phases.

not too high spontaneous polarization, good chemical stability, due to the absence of the ester group in achiral terminal chain, and compatibility of components, which were the major disadvantages of previously reported **W-212B3A** mixture [33]. However, they exhibit two times higher rotational viscosity but also much lower melting point than the last reported materials for DHF mode [31]. So, that means they can work slower but at lower temperatures. Further work is now underway to investigate in details the electro-optic response of developed mixtures in DHF mode. It is possible to conclude that excellent chemical stability and compatibility of components as well as moderate values of spontaneous polarization adds another great deal to these FLCs mixtures for application in *opto-electronics* and *photonics*.

Acknowledgements

Authors are greatly acknowledged the financial support from the following research projects: Czech Science Foundation CSF 19-03564S, POIG.01.03.01-14-016/08 and PBS 23-895. Two authors (A.B and P.S.) would like to acknowledge also the specific contribution of the COST Action CA17139. Financial support from the grants NKFIH PD 121019 and FK 125134 are acknowledged.

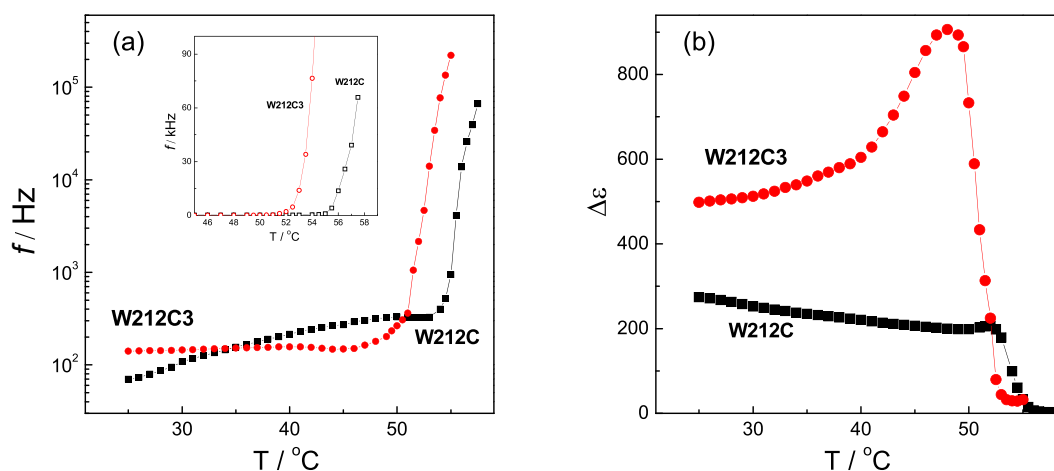


Fig. 10. Temperature dependence of (a) the relaxation frequency, $f(T)$, and (b) the dielectric strength, $\Delta\epsilon(T)$, at zero applied bias voltage for **W212C** and **W212C3** mixtures as indicated. The inset in (a) shows the behaviour of the relaxation frequency in the vicinity of the SmA*-SmC* phase transition.

References

- J.P.F. Lagerwall, G. Scalia, A new era for liquid crystal research: applications of liquid crystals in soft matter nano-, bio- and microtechnology, *Curr. Appl. Phys.* 2 (2012) 1387–1412, <https://doi.org/10.1016/j.cap.2012.03.019>.
- J.P.F. Lagerwall, F. Giesselmann, Current topics in smectic liquid crystal research, *Chem. Phys. Chem.* 7 (2006) 20–45, <https://doi.org/10.1002/cphc.200500472>.
- K. Kurp, M. Czerwiński, M. Tykarska, Ferroelectric compounds with chiral (S)-1-methylheptyloxycarbonyl terminal chain – their miscibility and a helical pitch, *Liq. Cryst.* 42 (2) (2015) 248–254, <https://doi.org/10.1080/02678292.2014.982222>.
- Ł. Szczuciński, R. Dąbrowski, S. Urban, K. Garbat, M. Filipowicz, J. Dziaduszek, M. Czerwiński, Synthesis, mesogenic and dielectric properties of fluorosubstituted isothiocyanatoterphenyls, *Liq. Cryst.* 42 (2015) 1706–1729, <https://doi.org/10.1080/02678292.2015.1070924>.
- A. Bubnov, V. Novotná, V. Hamplová, M. Kašpar, M. Glogarová, Effect of multilactate chiral part of liquid crystalline molecule on mesomorphic behaviour, *J. Mol. Struct.* 892 (2008) 151–157, <https://doi.org/10.1016/j.molstruc.2008.05.016>.
- A. Bubnov, V. Hamplová, M. Kašpar, P. Vaněk, D. Pocięcha, M. Glogarová, New ferroelectric liquid crystalline substances with lateral groups in the core, *Mol. Cryst. Liq. Cryst.* 366 (2001) 547–556, <https://doi.org/10.1080/10587250108023995>.
- V. Novotná, V. Hamplová, A. Bubnov, M. Kašpar, M. Glogarová, N. Kapernaum, S. Bezner, F. Giesselmann, First photoresponsive liquid-crystalline materials with small layer shrinkage at the transition to the ferroelectric phase, *J. Mater. Chem.* 19 (2009) 3992–3997, <https://doi.org/10.1039/b821738f>.
- A. Poryvai, A. Bubnov, D. Pocięcha, J. Svoboda, M. Kohout, The effect of terminal n-carboxylate chain length on self-assembling and photosensitive properties of lactic acid derivatives, *J. Mol. Liq.* 275 (2019) 829–838, <https://doi.org/10.1016/j.molliq.2018.11.058>.
- M. Żurowska, M. Szala, J. Dziaduszek, P. Morawiak, A. Bubnov, Effect of lateral fluorine substitution far from the chiral center on mesomorphic behaviour of highly tilted antiferroelectric (S) and (R) enantiomers, *J. Mol. Liq.* 267 (2018) 504–510, <https://doi.org/10.1016/j.molliq.2017.12.114>.
- A. Bubnov, V. Hamplová, M. Kašpar, A. Vajda, M. Stojanović, D. Obadović, N. Éber, K. Fodor-Csorba, Thermal analysis of binary liquid crystalline mixtures: system of bent core and calamitic molecules, *J. Therm. Anal. Calor.* 90 (2007) 431–441, <https://doi.org/10.1007/s10973-006-7913-7>.
- A. Bubnov, M. Tykarska, V. Hamplová, K. Kurp, Tuning the phase diagrams: the miscibility studies of multilactate liquid crystalline compounds, *Phase Transit.* 89 (2016) 885–893, <https://doi.org/10.1080/01411594.2015.1087523>.
- A. Bubnov, N. Podoliak, V. Hamplová, P. Tomášková, J. Havlíček, M. Kašpar, Eutectic behaviour of binary mixtures composed of two isomeric lactic acid derivatives, *Ferroelectrics* 495 (2016) 105–115, <https://doi.org/10.1080/00150193.2016.1136776>.
- J. Fitas, M. Marzec, M. Szymkowiak, T. Jaworska-Gołąb, A. Deptuch, M. Tykarska, K. Kurp, M. Żurowska, A. Bubnov, Mesomorphic, electro-optic and structural properties of binary liquid crystalline mixtures with ferroelectric and antiferroelectric liquid crystalline behaviour, *Phase Transit.* 91 (2018) 1017–1026, <https://doi.org/10.1080/01411594.2018.1506883>.
- A. Iwan, A. Sikora, V. Hamplová, A. Bubnov, AFM study of advanced composite materials for organic photovoltaic cells with active layer based on P3HT: PCBM and chiral photosensitive liquid crystalline dopants, *Liq. Cryst.* 42 (2015) 964–972, <https://doi.org/10.1080/02678292.2015.1011243>.
- R.K. Shukla, K.K. Raina, V. Hamplová, M. Kašpar, A. Bubnov, Dielectric behaviour of the composite system: multiwall carbon nanotubes dispersed in ferroelectric liquid crystal, *Phase Transit.* 84 (2011) 850–857, <https://doi.org/10.1080/01411594.2011.558300>.
- A. Bubnov, A. Iwan, M. Cigl, B. Boharewicz, I. Tazbir, K. Wójcik, A. Sikora, V. Hamplová, Photosensitive self-assembling materials as functional dopants for organic photovoltaic cells, *RSC Adv.* 6 (2016) 11577–11590, <https://doi.org/10.1039/C5RA23137J>.
- R.K. Shukla, A. Chaudhary, A. Bubnov, K.K. Raina, Multiwalled carbon nanotubes – ferroelectric liquid crystals nanocomposites: effect of cell thickness and dopant concentration on electro-optic and dielectric behaviour, *Liq. Cryst.* 45 (2018) 1672–1681, <https://doi.org/10.1080/02678292.2018.1469170>.
- N.A. Clark, S.T. Lagerwall, Submicrosecond bistable electro-optic switching in liquid crystals, *Appl. Phys. Lett.* 36 (1980) 899–901, <https://doi.org/10.1063/1.91359>.
- A. Bubnov, C. Vacek, M. Czerwiński, T. Vojtylova, W. Piecek, V. Hamplova, Design of polar self-assembling lactic acid derivatives with the keto group and sub-micrometre helical pitch, *Beilstein J. Nanotech.* 9 (2018) 333–341, <https://doi.org/10.3762/bjnano.9.33>.
- V. Swaminathan, V.P. Panov, Yu.P. Panarin, S.P. Sreenilayam, J.K. Vij, A. Panov, D. Rodriguez-Lojo, P.J. Stevenson, E. Gorecka, The effect of chiral doping in achiral smectic liquid crystals on the de Vries characteristics: smectic layer thickness, electro-optics and birefringence, *Liq. Cryst.* 45 (4) (2018) 513–521, <https://doi.org/10.1080/02678292.2017.1359694>.
- D. Węglowska, P. Perkowski, M. Chrunik, M. Czerwiński, The effect of dopant chirality on the properties of self-assembling materials with a ferroelectric order, *Phys. Chem. Chem. Phys.* 20 (14) (2018) 9211–9220, <https://doi.org/10.1039/c8cp01004h>.
- D. Węglowska, P. Perkowski, W. Piecek, M. Mrukiewicz, R. Dąbrowski, The effect of the octan-3-yloxy and the octan-2-yloxy chiral moieties on the mesomorphic properties of ferroelectric liquid crystals, *RSC Adv.* 5 (99) (2016) 81003–81012, <https://doi.org/10.1039/c5ra14903g>.
- J. Fünfschilling, M. Schadt, Fast responding and highly multiplexible distorted helix ferroelectric liquid-crystal displays, *J. Appl. Phys.* 66 (1989) 3877–3882, <https://doi.org/10.1063/1.344452>.
- L.A. Beresnev, V.G. Chigrinov, D.I. Dergachev, E.P. Poshidaev, J. Fünfschilling, M. Schadt, Deformed helix ferroelectric liquid crystal display: a new electrooptic mode in ferroelectric chiral smectic C* liquid crystals, *Liq. Cryst.* 5 (1989) 1171–1177, <https://doi.org/10.1080/02678298908026421>.
- I. Abdulhalim, G. Moddel, Electrically and optically controlled light modulation and color switching using helix distortion of ferroelectric liquid crystals, *Mol. Cryst. Liq. Cryst.* 200 (1991) 79–101, <https://doi.org/10.1080/00268949108044233>.
- E. Pozhidaev, S. Torgova, M. Minchenko, C. Augusto Refosco Yednak, A. Strigazzi, E. Miraldi, Phase modulation and ellipticity of the light transmitted through a smectic C* layer with short helix pitch, *Liq. Cryst.* 37 (2010) 1067–1081, <https://doi.org/10.1080/02678292.2010.486482>.
- A.D. Kiselev, E.P. Pozhidaev, V.G. Chigrinov, H.S. Kwok, Polarization-gratings approach to deformed-helix ferroelectric liquid crystals with subwavelength pitch, *Phys. Rev. E* 83 (2011), 031703, <https://doi.org/10.1103/PhysRevE.83.031703>.
- A.D. Kiselev, Phase modulation of mixed polarization states in deformed helix ferroelectric liquid crystals, *J. Mol. Liq.* 267 (2018) 253–265, <https://doi.org/10.1016/j.molliq.2017.12.126>.
- S.P. Kotova, S.A. Samagin, E.P. Pozhidaev, A.D. Kiselev, Light modulation in planar aligned short-pitch deformed-helix ferroelectric liquid crystals, *Phys. Rev. E* 92 (2015), 062502, <https://doi.org/10.1103/PhysRevE.92.062502>.
- V.V. Kesaev, A.D. Kiselev, E.P. Pozhidaev, Modulation of unpolarized light in planar-aligned subwavelength-pitch deformed-helix ferroelectric liquid crystals, *Phys. Rev. E* 95 (2017), 032705, <https://doi.org/10.1103/PhysRevE.95.032705>.
- V. Mikhailenko, A. Krivoshey, E. Pozhidaev, E. Popova, A. Fedoryako, S. Gamzaeva, V. Barbashov, A.K. Srivastava, H.S. Kwok, V. Vashchenko, The nano-scale pitch ferroelectric liquid crystal materials for modern display and photonic application employing highly effective chiral components: Trifluoromethylalkyl diesters of p-terphenyldicarboxylic acid, *J. Mol. Liq.* 281 (2019) 186–195, <https://doi.org/10.1016/j.molliq.2019.02.047>.
- Q. Guo, Z. Brodzki, E.P. Pozhidaev, F. Fan, V.G. Chigrinov, H.S. Kwok, L. Silvestri, F. Ladouceur, Fast electrooptical mode in photoaligned reflective deformed helix

- ferroelectric liquid crystal cells, *Opt. Lett.* 37 (12) (2012) 2343–2345, <https://doi.org/10.1364/OL.37.002343>.
- [33] K. Kurp, M. Czerwiński, M. Tykarska, A. Bubnov, Design of advanced multicomponent ferroelectric liquid crystalline mixtures with submicrometre helical pitch, *Liq. Cryst.* 44 (4) (2017) 748–756, <https://doi.org/10.1080/02678292.2016.1239774>.
- [34] A. Fukuda, Pretransitional effect in AF-F switching: To suppress it or to enhance it, that is my question about AFLCDs, *Proc. 15th Asia Display*, Hamamatsu, 1995, vol. 61, The Institute of Television Engineers of Japan, Tokyo, 1995, S6–1.
- [35] S. Inui, N. Imura, T. Suzuki, H. Iwane, K. Miyachi, Y. Takanishi, A. Fukuda, Thresholdless antiferroelectricity in liquid crystals and its application to displays, *J. Mater. Chem.* 6 (1996) 671–673, <https://doi.org/10.1039/JM9960600671>.
- [36] M. Czerwiński, M. Tykarska, Helix parameters in bi- and multicomponent mixtures composed of orthoconic antiferroelectric liquid crystals with three ring molecular core, *Liq. Cryst.* 41 (6) (2014) 850–860, <https://doi.org/10.1080/02678292.2014.884248>.
- [37] Z. Raszewski, J. Kędzierski, P. Perkowski, W. Piecek, J. Rutkowska, S. Kłosowicz, J. Zieliński, Refractive indices of the MHPB (H) PBC and MHPB (F) PBC antiferroelectric liquid crystals, *Ferroelectrics* 276 (2002) 289–300, <https://doi.org/10.1080/00150190214411>.
- [38] W. Kuczyński, S.T. Lagerwall, M. Matuszczyk, K. Skarp, B. Stebler, J. Wahl, Fast-switching low-temperature liquid crystal mixture, *Mol. Cryst. Liq. Cryst.* 146 (1987) 173–187, <https://doi.org/10.1080/00268948708071812>.
- [39] M. Tykarska, M. Czerwiński, J. Miskurka, Influence of temperature and terminal chain length on helical pitch in homologue series nH6Bi, *Liq. Cryst.* 37 (2010) 487–495, <https://doi.org/10.1080/02678291003686880>.
- [40] W. Drzewiński, K. Czupryński, R. Dąbrowski, M. Neubert, New Antiferroelectric compounds containing partially fluorinated terminal chains. Synthesis and Mesomorphic properties, *Mol. Cryst. Liq. Cryst.* 328 (1999) 401–410, <https://doi.org/10.1080/10587259908026083>.
- [41] P.K. Mandal, B.R. Jaishi, W. Haase, R. Dąbrowski, M. Tykarska, P. Kula, Optical microscopy, DSC and dielectric relaxation spectroscopy studies on a partially fluorinated ferroelectric liquid crystalline compound MHPO (13F) BC, *Phase Transit.* 79 (2006) 223–235, <https://doi.org/10.1080/01411590500500724>.
- [42] M. Tykarska, R. Dąbrowski, J. Przedmojski, W. Piecek, K. Skrzypek, B. Donnio, D. Guillon, Physical properties of two systems with induced antiferroelectric phase, *Liq. Cryst.* 35 (2008) 1053–1059, <https://doi.org/10.1080/02678290802364004>.
- [43] M. Żurowska, R. Dąbrowski, J. Dziaduszek, K. Garbat, M. Filipowicz, M. Tykarska, W. Rejmer, K. Czupryński, A. Spadło, N. Bennis, J.M. Oton, Influence of alkoxy chain length and fluorosubstitution on mesogenic and spectral properties of high tilted antiferroelectric esters, *J. Mater. Chem.* 21 (2011) 2144–2153, <https://doi.org/10.1039/C0JM02015J>.
- [44] W. Piecek, P. Perkowski, Z. Raszewski, P. Morawiak, M. Żurowska, R. Dąbrowski, K. Czupryński, Long pitch orthoconic antiferroelectric binary mixture for display applications, *Mol. Cryst. Liq. Cryst.* 525 (2010) 160–172, <https://doi.org/10.1080/15421401003796223>.
- [45] M. Czerwiński, M. Tykarska, R. Dąbrowski, A. Chełstowska, M. Żurowska, R. Kowderziej, L.R. Jaroszewicz, The influence of structure and concentration of cyano-terminated and terphenyl dopants on helical pitch and helical twist sense in orthoconic antiferroelectric mixtures, *Liq. Cryst.* 39 (2012) 1498–1502, <https://doi.org/10.1080/02678292.2012.723047>.
- [46] A. Chełstowska, M. Czerwiński, M. Tykarska, N. Bennis, The influence of antiferroelectric compounds on helical pitch of orthoconic W-1000 mixture, *Liq. Cryst.* 41 (6) (2014) 812–820, <https://doi.org/10.1080/02678292.2014.885601>.
- [47] W. Piecek, A. Bubnov, P. Perkowski, P. Morawiak, K. Ogrodnik, W. Rejmer, M. Żurowska, V. Hamplová, M. Kašpar, An effect of structurally non compatible additive on the properties of a long pitch antiferroelectric orthoconic mixture, *Phase Transit.* 83 (2010) 551–563, <https://doi.org/10.1080/01411594.2010.499496>.
- [48] K. Skarp, Rotational viscosities in ferroelectric smectic liquid crystals, *Ferroelectrics* 84 (1988) 119–142, <https://doi.org/10.1080/00150198808016217>.
- [49] E.P. Pozhidaev, V.V. Vashchenko, V.V. Mikhailenko, A.I. Krivoshey, V.A. Barbashov, L. Shi, A.K. Srivastava, V.G. Chigrinov, H.S. Kwok, Ultrashort helix pitch antiferroelectric liquid crystals based on chiral esters of terphenyldicarboxylic acid, *J. Mater. Chem. C* 4 (2016), 10339, <https://doi.org/10.1039/C6TC04087J>.